Comparison of RCS calculations of Complex Targets by using FDTD –Based Virtual Tools

B.Nagarjuna
M.Tech DE&CS Vasireddy Venkatadri Institute of Technology Numbur AP-India,
Mail:naga.8123@gmail.com

***Abstract*—:Radar cross section is one of the key parameters in the detection of targets. It is used to describe the amount of scattered power from a target towards the radar. A novel, accelerated, and parallelized Finite-Difference Time-Domain (FDTD) based radar cross section (RCS) prediction tool, MGL-FastRCS, is used for different complex targets are simulated via both the finite difference time domain method and the Method of Moments (MOM).The virtual RCS prediction tool that was introduced in previous work is used for these investigations. The virtual tool automatically creates the discrete FDTD model of the target under investigation and performs the FDTD RCS analysis. It also automatically constructs a MoM wire grid model of the targets; therefore, it is also possible to compare FDTD results against the MoM- based data. Another FDTD-based RCS Virtual prediction tool,MGL-RCS, was designed in such a way as to automatically constructs a wire-grid model of the structure under investigation.**

***Keywords*— : Scattering; diffraction; radar; radar cross section; RCS; RCS prediction; Finite-Difference Time-Domain; FDTD; virtual tool design; graphics processing unit; parallel processing.**

I.INTRODUCTION

When radar illuminates a target, RCS is a measure of scattered power by an incident electromagnetic wave. It is measured in a given direction. It doesn't depend on the distance of the target from the source as it is normalized with respect to power density of the incident wave. In RCS measurement, it is not required to know the position of the receiver. The scattered echo is usually spherical in nature. RCS is used to obtain target characteristics, transmitter power, receiver sensitivity, position of transmitter and receiver distance. Sometimes it also represents an echo area. In fact, it is a function of frequency, aspect angle, shape of the target, position of the transmitter and receiver relative to the target geometry, material, and angular orientation of the target relative to the transmitter and the receiver and antenna polarization[2]. Three-dimensional models of surface and/or air vehicles, saved in files in the **3DS** format (the ***3D** Studio* file format; see http://www.autodesk.com for details), can be used as radar targets. Near-EM scattered fields around the target, caused by an incident Gaussian plane wave hitting the target from a specified direction, can be simulated using a three dimensional numerical FDTD model. EM transient scattering may also be recorded in a specified file as a video clip. Far fields can be extrapolated and stored via the application of the equivalence principle. Bistatic RCS patterns can be plotted using the discrete Fourier transformation (DFT) on the stored time-domain EM scattered data. The Finite-Difference Time-Domain (FDTD) method is a popular three-dimensional (3D) EM numerical method for solving a wide range of problems

Based on the discretization of Maxwell's equations directly in the time domain, the FDTD method requires a large amount of data processing and long computing times. To overcome these problems, parallel FDTD algorithms have been developed. Parallel processing in numerical simulations is based on dividing a computer code into a number of subroutines, distributing the task among a number of computers, and executing all in parallel. Parallelization may be on the hardware level, the software level, or both. Hardware-level parallelization requires alternative processor designs as well computer optimization *MGL-FastRCS* has been parallelized with *OpenMP* and *CUDA* for high-performance computing with multiple cores and GPUs. The RCS prediction tool can be used to create three-dimensional targets from canonical blocks, such as a rectangular prism, cone, cylinder, sphere, and toroid; or three dimensional models of surface and/or air vehicles saved in 3DS-format files can be used as radar targets. Near EM scattered fields around the target, caused by an incident Gaussian plane wave hitting the target from a specified direction, can be simulated using a three-dimensional numerical FDTD model. Far fields can be extrapolated and stored via the application of the Equivalence Principle. Bistatic RCS patterns can be plotted using the discrete Fourier transformation (DFT) applied to the stored time-domain EM scattered data.

II.THE MGL-FASTRCS VIRTUAL TOOL

A. RCS Definitions

The definition of RCS has two view points, one is based on electromagnetic scattering theory, and other is based on the view of radar measurement [24]. Both basic concepts are unified, that is 4π times ratio between targets receive direction scattering power and emission direction plane wave power density in per unit solid angle. The RCS, σ, is calculated and/or measured from the target-scattered fields caused by an incident plane wave hitting the target from a specified direction.[19]

$$\sigma = \lim_{R\to\infty}\left\{4\pi R^2 \frac{|E_s|^2}{|E_i|^2}\right\},\ E_{i,s} = E_\theta \text{ or } E_\varphi, \qquad (1)$$

The three RCS frequency regimes where qualitative as well as quantitative differences occur are:

(i) low frequencies (the *Rayleigh regime*), where the tar get's (*longest*) dimension (l) is much less than the radar wavelength ($l << \lambda$);
(ii) medium frequencies (the *resonance regime*), where the target's dimension and the radar wavelength are of the same order ($l \approx \lambda$);
(iii) high frequencies (the *optical regime*), where the target dimension is very large compared to the radar wavelength ($l >> \lambda$).

The standard FDTD procedure for RCS and antenna simulations is as follows[20,21]:

- The discrete target or antenna model is located at the center of the three dimensional FDTD volume .
- User-specified data are fed to the main routine. This includes polarization, source bandwidth, number of time steps, polar-diagram parameters for the radiation characteristics.
- The source is a broadband pulse for antenna excitations, but it is a pulsed Gaussian plane wave for RCS simulations.
- The near-to-far-field transformation is based on the accumulation of the far-zone vector potentials due to the tangential electric and magnetic fields on a virtual, closed surface, surrounding the object under investigation at each time step.
- The near-to-far-field transformation process is repeated for every other angular direction.

B. The MGL-FastRCS User Manual

The package contains three executable files: MGLFastRCS, MGL-cudaFDTD, and MGL-PLOT. The first part consists of the d*esign wizard*, *visualization window*, *file management*, and *calculation of RCS patterns.* The program can automatically be run inside the *MGL-FastRCS* module if *OpenMP* parallization is preferred; otherwise, the second module, *MGL-cudaFDTD*, which uses the graphics card, must be run separately. Note that *MGL-cudaFDTD* must be run after the creation of the RCS.PAR fi le. It can be used to design any kind of a PEC target using basic blocks such as a rectangular prism, cone, cylinder, sphere, etc. Moreover, it contains a powerful tool that creates discrete models from graphics-file images. A collection of pre-designed surface and air targets stored in 3DS (3D Studio file, visit www.autodesk.com for details) format files are also supplied. The *MGL-FastRCS* module can create discrete FDTD and *NEC* models and save them in PAR.RCS and PAR.NEC files. Time and frequency-domain two-dimensional graphs can be plotted using the second module, *MGL-PLOT[1]*.

The front panel of the *MGL-FastRCS* package is given in Figure 1. At top, besides the regular buttons, are located object design buttons. Any target can be designed with the help of rectangular, cylindrical, conical, spherical, and toroidal blocks. The user can not only create original targets from these basic blocks, but can also insert custom-made images. The models are in 3DS format and can be downloaded from various Internet sites. The two blocks on the right are used for operational parameters and model creation. In the Operational Parameters block, the incident field and RCS scan parameters are specified. Only a vertical or horizontal scan is possible with this package.

The scan angle is the angular resolution and is supplied by the user. The number of time steps, i.e., the FDTD simulation period is also supplied from this block (it should be noted that with the structural parameters chosen in this package, 600 to 1000 time steps are enough for the time-domain simulations). In the Dimensional Parameters block, the sizes of the target are displayed. The user only sup plies the cell size (Delta) in this block. Once this is given, the number of cells along each direction is automatically displayed.

MGL-FastRCS, or the second module, *MGL-cudaFDTD*, calculates near fields in the time domain using the FDTD method, and extrapolates far-scattered fields all around the target on a specified observation (either vertical or horizontal) plane with a given angular resolution. It also plots a number of angular RCS patterns at user-supplied frequencies by applying the discrete Fourier transform to the FDTD simulation data. The operational and target parameters are read from RCS.PAR, and the output is recorded in a fi le named PLAIN.TXT. The output file contains multiple columns for the angle of scattering (θs and ϕs), the theta and phi components of the scattered electric field, and the rectangular components of the near electric field (Ex , Ey , and Ez) at a point.

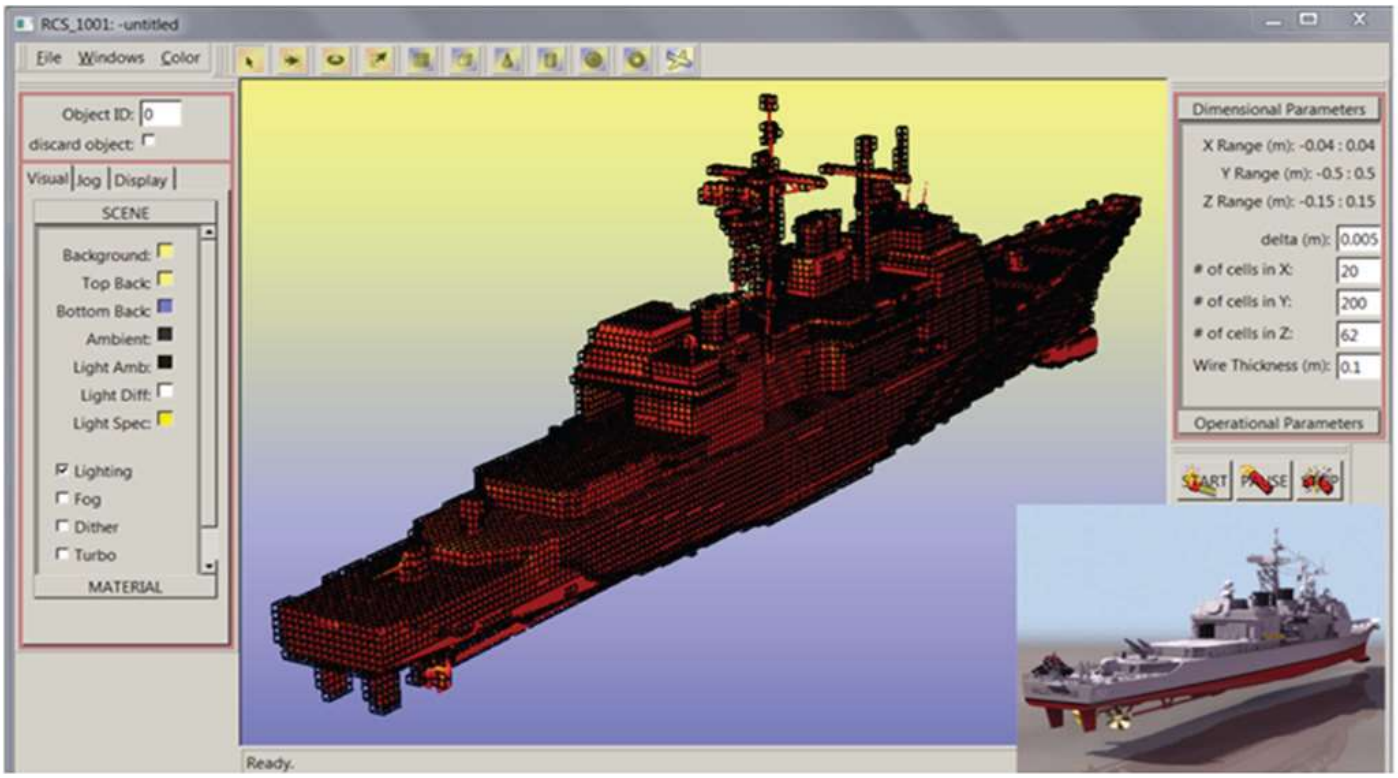

Figure 1a. The front panel of the *MGL-FastRCS* package.

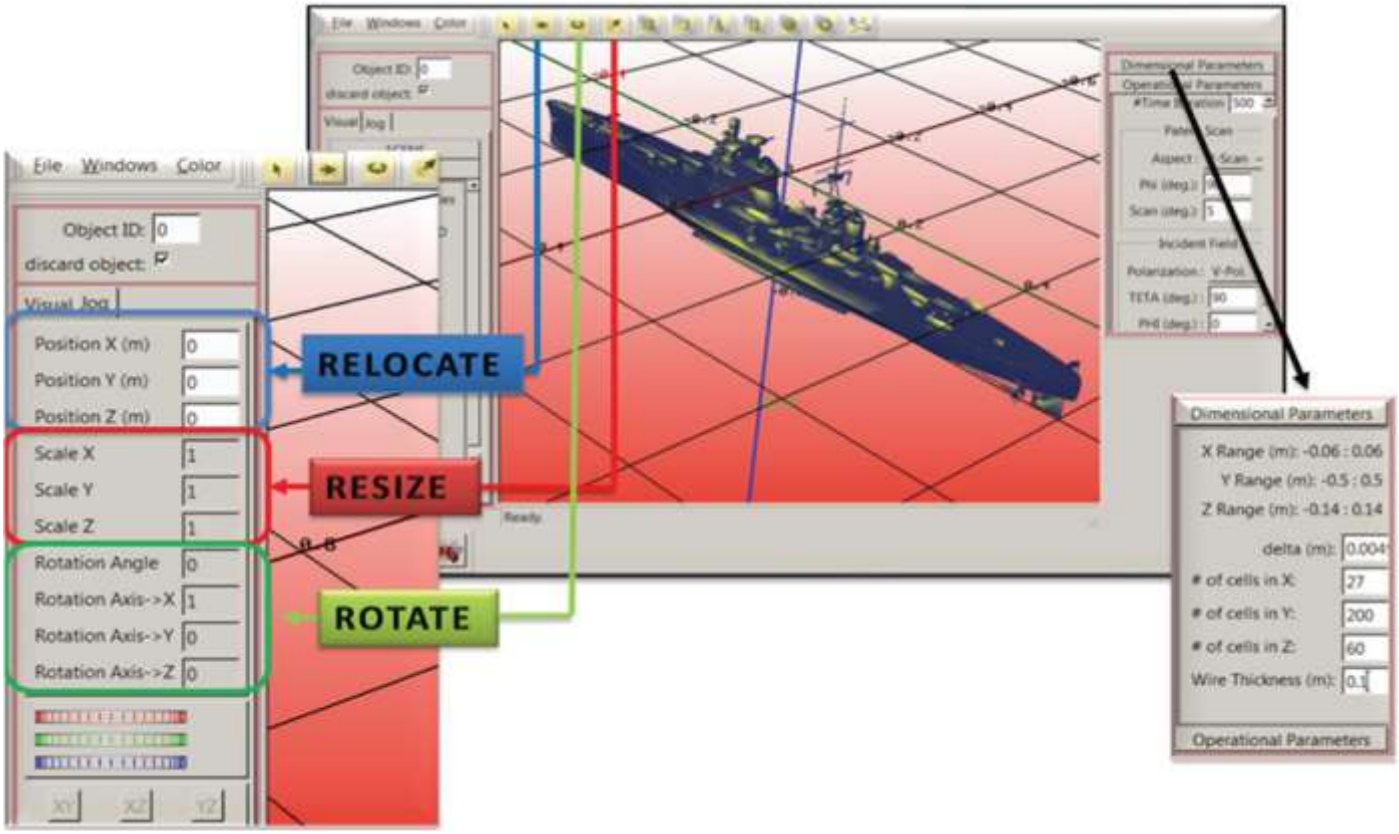

Figure 1b. The dimensional parameters are shown on the right block

The last module of the virtual tool is *MGL-PLOT*, which may be used to produce two-dimensional plots using the output file PLAIN.TXT. The user may plot time variations of the scattered fields along a specified direction, or RCS, as a function of frequency for both the monostatic and bistatic cases.

The buttons START, PAUSE, and STOP are the runtime control buttons of the package. Once the START button is pressed, the FDTD simulation begins. The user then observes the incident field hitting the target from the specified direction, and the transient scattered fields all around the target, on a specified observation plane.

III. RCS CALCULATIONS OF DIFFERENT COMPLEX TARGETS

In general, the RCS of a target may be given as (i) mono-RCS as a function of frequency for a specified illumination and the same scattering directions (this is called bi-RCS as a function of frequency if these directions are different), (ii) angular mono- or bistatic RCS patterns at a given frequency (a monostatic pattern is obtained by illuminating the target consecutively all around, and recording only backscattered fields; a bistatic RCS pattern is obtained by illuminating the target once from a specified direction and recording scattered fields all around)[5].

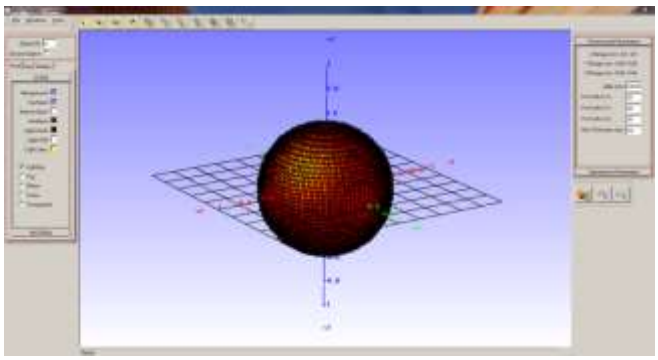

Figure 2a.A discrete model for Sphere.

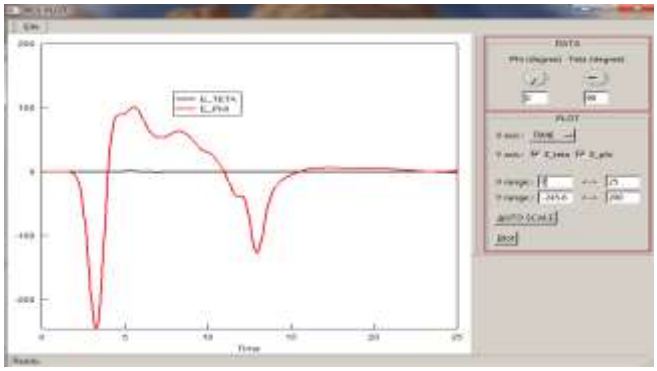

Figure 2b.A plot of the monostatic RCS as a function of Time for the Sphere when the angle of illumination and scatter were same (θi=θs= 90° φi=φs= 0°); the polarization was horizontal (i.e., the $\sigma_{\varphi\varphi}$ case)

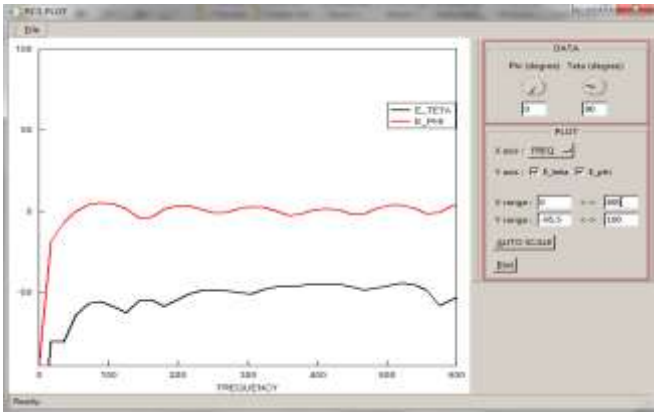

Figure 2c..A plot of the bistatic RCS as a function of frequency for the Sphere shown when the angle of illumination and scatter were same (θi=θs= 90° φi=φs= 0°); the polarization was horizontal (i.e., the $\sigma_{\varphi\varphi}$ case)

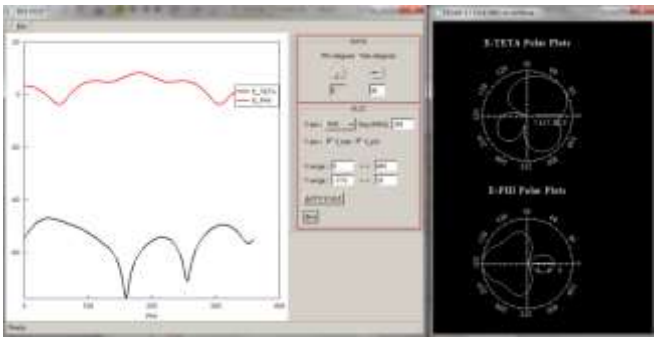

Figure 2d.The angular bistatic RCS pattern of sphere simulated with FDTD result at f=200 MHz; $\theta_i=90^0$,$\varphi_i=0^0$.

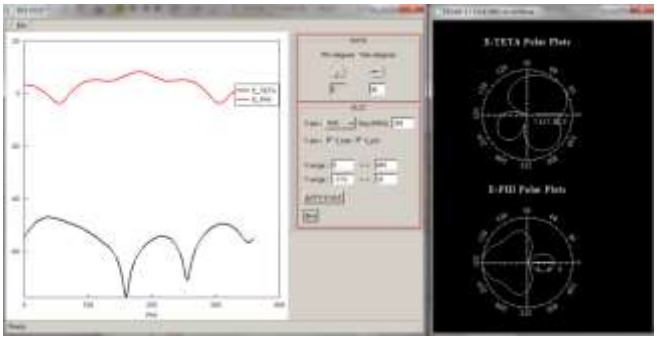

Figure 2e.The angular bistatic RCS pattern of sphere simulated with FDTD result at f=500 MHz; $\theta_i=90^0$,$\varphi_i=0^0$.

Figure 2a shows the discrete model for Sphere. A plot of the monostatic RCS as a function of Time for the Sphere when the angle of illumination and scatter were same (θi=θs= 90° φi=φs= 0°); the polarization was horizontal is shown in Figure 2b.The angular bistatic RCS patterns simulated with FDTD at f=200 MHz and f=500 MHz are shown in Figure 2d and Figure 2e.With the help of parallelization and the high-soeed grid technique used in this virtual tool and complex realistic targets can be discretized in this virtual tool.

A discrete model for an F16 flighter jet is shown in Figure 3a.The angular bistatic RCS patterns simulated with FDTD at *f*=20MHz and *f*=60MHz are shown in Figure3e and Figure 3f. The near fields over a horizontal slice around the target simulated inside the specified FDTD volume (incident field was phi polarized, i.e., the electric field was parallel to the fuselage of the airplane).

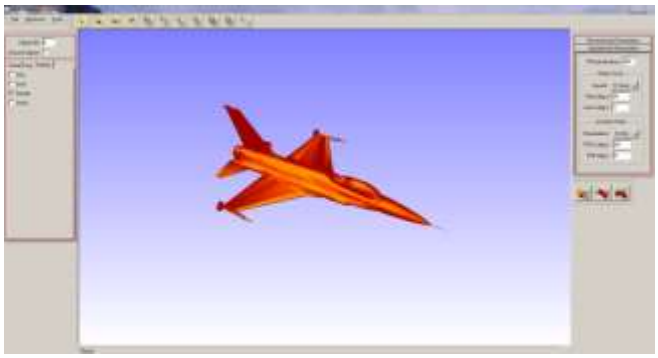

Figure 3a. A discrete model for an F16 fighter jet.

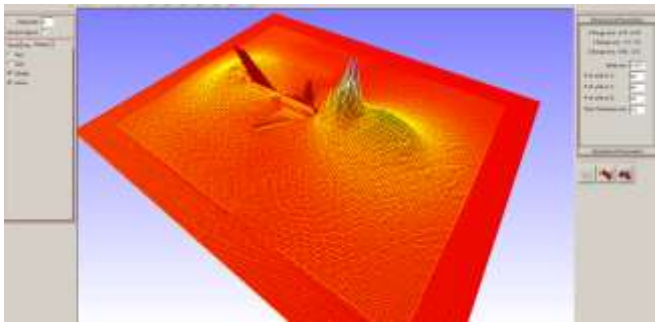

Figure 3b. The near fields over a horizontal slice around the target simulated inside the specified FDTD volume (incident field was phi polarized, i.e., the electric field was parallel to the fuselage of the airplane).

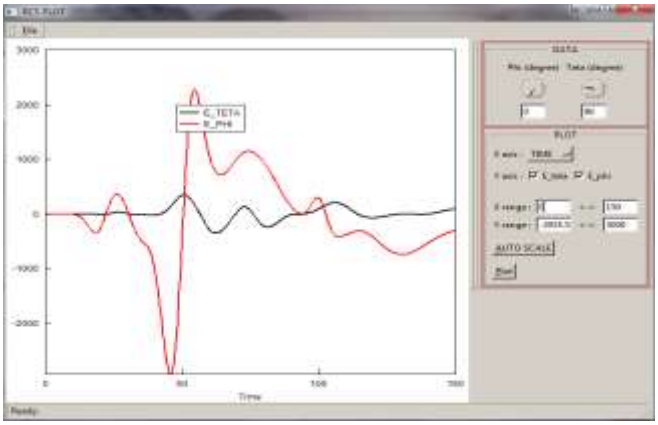

Figure 3c. A plot of the bistatic RCS as a function of Time for an F16 air craft.

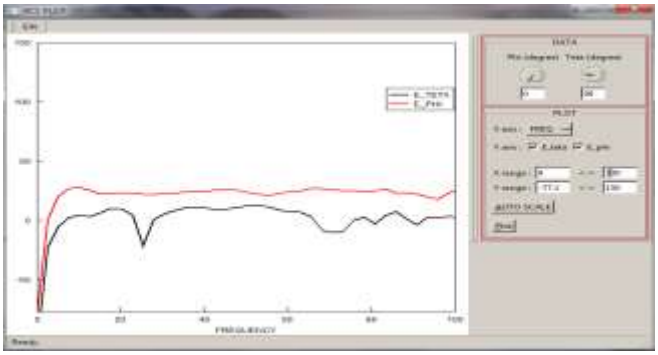

Figure 3d. A plot of the bistatic RCS as a function of Frequency for an F16 air craft.

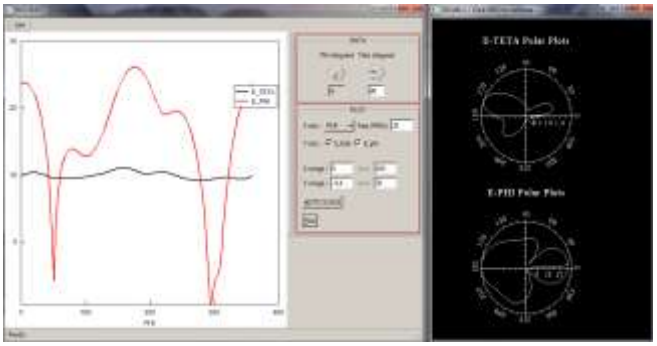

Figure 3e.The angular bistatic RCS pattern for an F16 air craft simulated with FDTD result at *f*=20 MHz; $\theta_i=90^0,\varphi_i=0^0$.

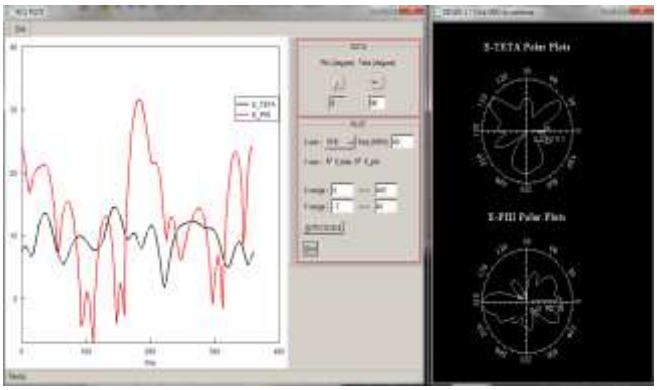

Figure 3f. The angular bistatic RCS pattern for an F16 air craft simulated with FDTD result *f*=60 MHz; $\theta_i=90^0,\varphi_i=0^0$.

The FDTD-based RCS prediction virtual tool ,MGL-RCS, is designed in a way to automate almost the whole RCS analysis procedure. It has a useful Graphical User Interface(GUI) with features like 3d visualization, real time rotate, pan and zoom

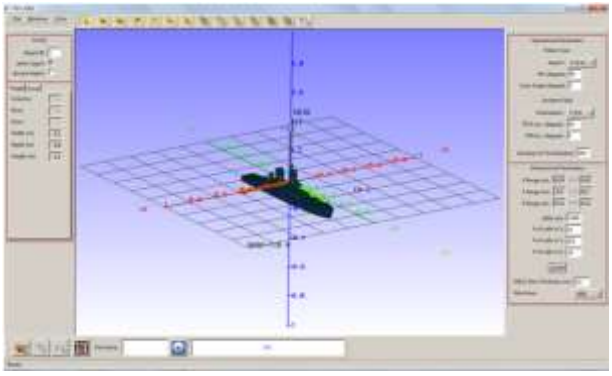

Figure 4a. A discrete model for Belknap.

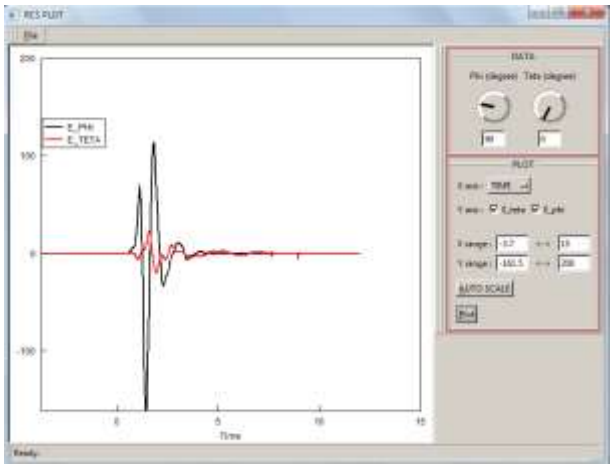

Figure 4b. RCS Plot for V scan at $\theta=90^0$ and $\varphi=0^0$.

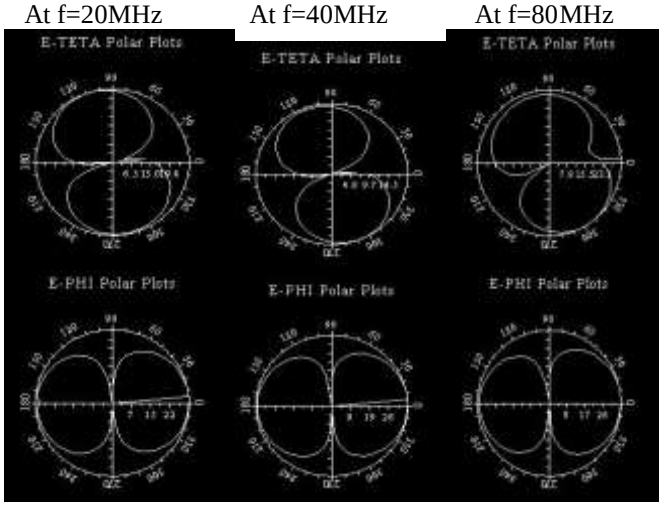

Figure 4c. Radiation Patterns for V Scan at different frequencies.

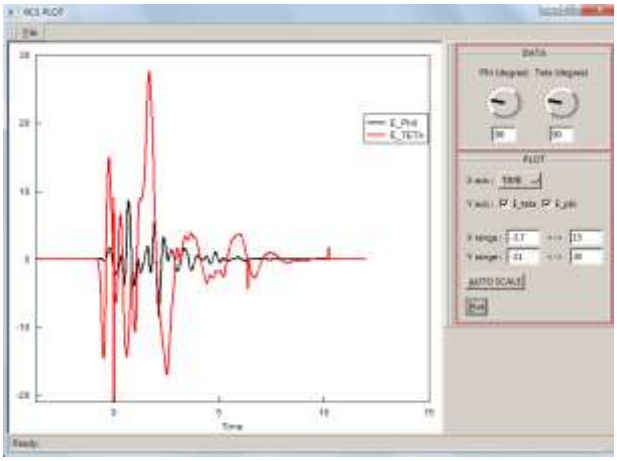

Figure 4d. RCS Plot for H scan at $\theta=90^0$ and $\varphi=0^0$.

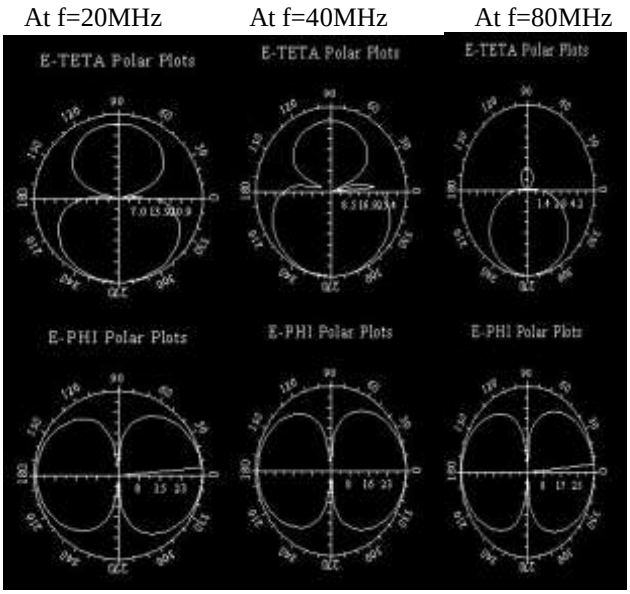

Figure 4e. . Radiation Patterns for H Scan at different frequencies.

The Discrete FDTD model of the Belknap target is shown in figure 4a.After wire gird model can be created from the FDTD gird. The second module is MGL-FDTD, calculates near – fields in the time domain using the FDTD method, and extrapolates far-scattered fields all around the target on a specified observation plane with a angular resolution. It also plots a number of angular RCS patterns at specified frequency .when applied vertical scan on the FDTD model we get RCS Plot with respect to time.RCS Plot for v scan at $\theta=90^0$ and $\varphi=0^0$ is shown in Figure 4b. The last module of the virtual tool MGL-PLOT may be used to produce 2D plots using output file. Radiation Patterns for V Scan at different frequencies at 20MHz,40MHz and 80MHz is shown in Figure 4c.Similarly for Radiation Patterns for H Scan at different frequencies at20MHz,40MHz and 80MHz is shown in Figure 4e.

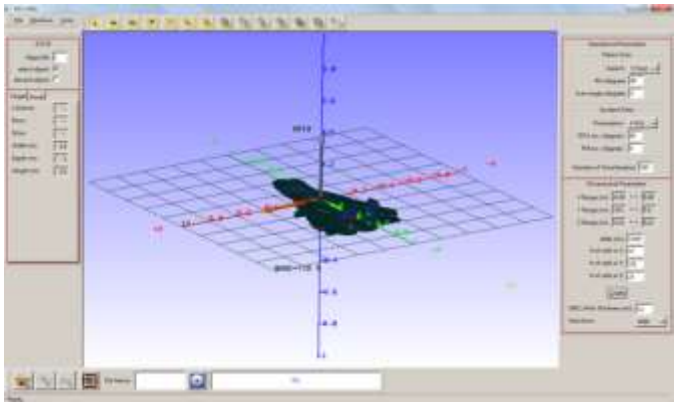

Figure 5a. A discrete model for F14

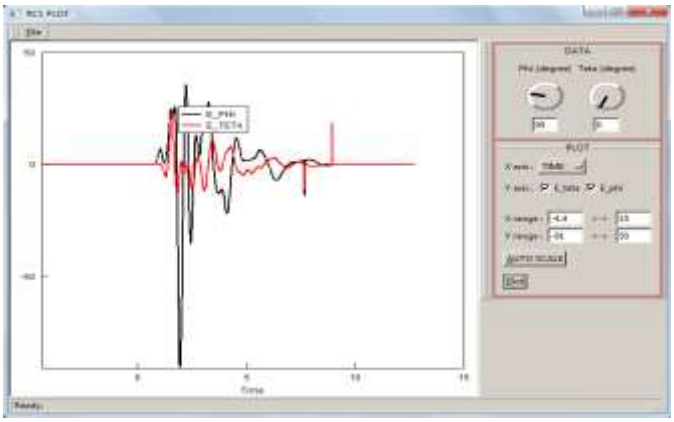

Figure 5b. RCS Plot for V scan at θ=90^0 and φ=0^0.

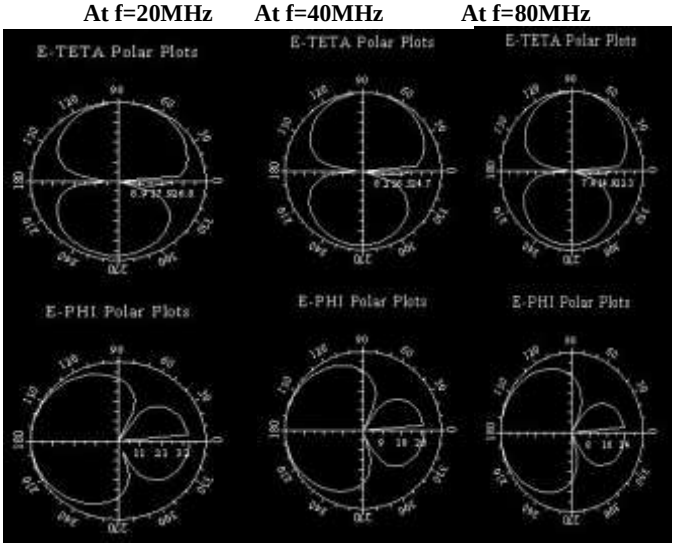

Figure 5c. Radiation Patterns for V Scan at different frequencies.

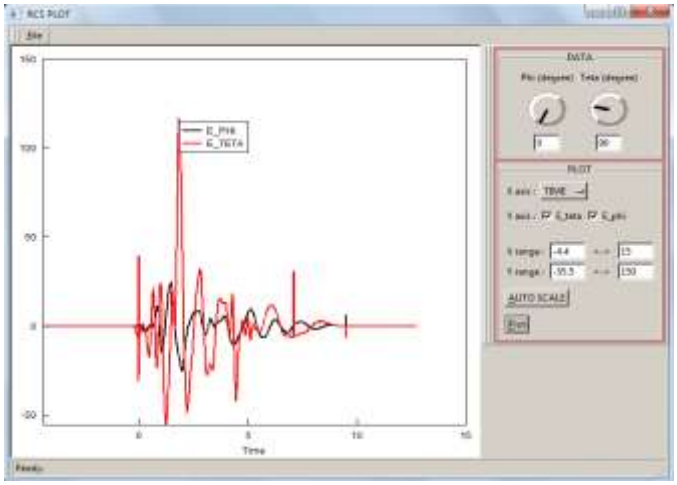

Figure 5d. RCS Plot for H scan at θ=90^0 and φ=0^0.

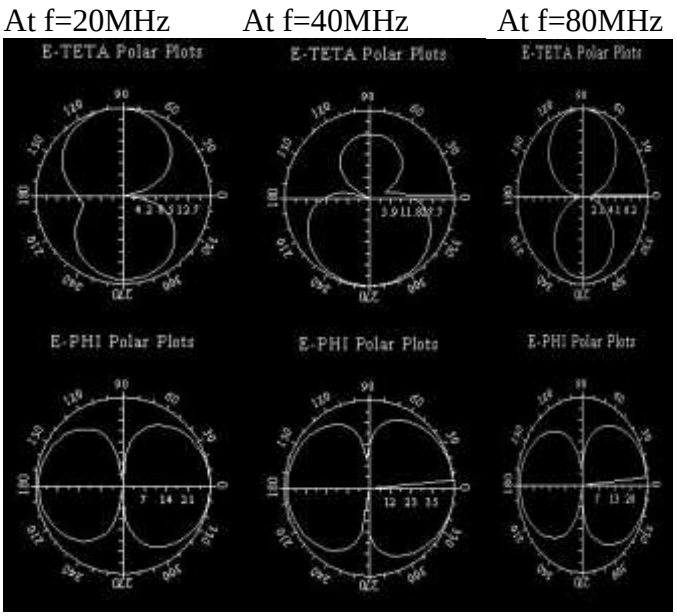

Figure 5e. Radiation Patterns for H Scan at different frequencies.

The Discrete FDTD model of the F14 target is shown in figure 5a. when applied vertical scan on the FDTD model we get RCS Plot with respect to time. when applied Horizontal scan on the FDTD model we get RCS Plot with respect to time RCS Plot for v scan at θ=90^0 and φ=0^0 is shown in Figure 4b. The last module of the virtual tool MGL-PLOT may be used to produce 2D plots using output file. Radiation Patterns for V Scan at different frequencies at 20MHz,40MHz and 80MHz is shown in Figure 4c.Similarly for Radiation Patterns for H Scan at different frequencies at20MHz,40MHz and 80MHz is shown in Figure 4e.

IV. CONCLUSION

A novel FDTD-based virtual analysis RCS prediction tool, MGL Fast RCS was used for any object having a 3DS graphics file can be imported, its discrete FDTD model is

automatically created for the specified set of parameters, and the final parameter file is created for the FDTD-based RCS simulations. In order to work on large-scale targets in a reasonable time, this program consists of parallel sections. If one has a CUDA-compatible GPU card, the MGL-cudaFDTD.exe module can be used for radarcross section predictions. Another program, named MGL-PLOT, can be used for visualizing time- and frequency-domain data on two-dimensional graphs, so users doesn't need to write any code scripts. It is possible to analyse a realistically large target within a reasonable time with the MGL-Fast RCS. So MGL-Fast RCS is much faster than the MGL-RCS package.

ACKNOWLEDGMENT

I Thank My project guide Prof. M.Y.Bhanumurthy for his valuable suggestions in preparing the manuscript.

REFERENCES

1. G. Cakir, M. Cakir, L. Sevgi,"An FDTD-based Parallel Virtual Tool for the RCS Calculations of Complex Targets," IEEE Antennas and Propagation Magazine Vol. 56, No. 5, pp:74-90, October 2014

2. K. S. Yee, "Numerical Solution of Initial Boundary Value Problems Involving Maxwell Equations," *IEEE Transactionson Antennas and Propagation*, **AP-14**, 3, 1966, pp. 302-307.

3. S. E. Krakiwsky, L. E. Turner, and M. M. Okoniewski, "Graphics Processor Unit (GPU) Acceleration of Finite-Difference Time-Domain (FDTD) Algorithm," Proc. 2004 InternationalSymposium on Circuits and Systems, 5, May 2004, pp.265-268.

4. S. E. Krakiwsky, L. E. Turner, and M. M. Okoniewski,"Acceleration of Finite-Difference Time-Domain (FDTD) Using Graphics Processor Units (GPU)," 2004 IEEE MTT-S International Microwave Symposium Digest, 2, June 2004, pp.1033-1036.

5. M. J. Inman, A. Z. Elsherbeni, and C. E. Smith "GPU Programming for FDTD Calculations," The Applied Computational Electromagnetics Society (ACES) Conference, 2005.

6. M. J. Inman and A. Z. Elsherbeni, "Programming VideoCards for Computational Electromagnetics Applications,"*IEEE Antennas and Propagation Magazine*, **47**, 6, December 2005, pp. 71-78.

7. M. J. Inman, A. Z. Elsherbeni, J. G. Maloney, and B. N. Baker, "Practical Implementation of a CPML Absorbing Boundary for GPU Accelerated FDTD Technique," The 23rdAnnual Review
of Progress in Applied Computational Electromagnetics Society, March 19-23, 2007.

8. S. Adams, J. Payne, and R. Boppana, "Finite Difference Time Domain (FDTD) Simulations Using Graphics Processors," Proceedings of the 2007 DoD High Performance Com putting Modernization Program Users Group (HPCMP) Con ference, 2007, pp. 334-338.

9. D. K. Price, J. R. Humphrey, and E. J. Kelmelis, "GPUbasedAccelerated 2D and3D FDTD Solvers," Physics and Simulation of Optoelectronic Devices XV, Proceedings of SPIE,6468, January 2007.

10. K.-H. Kim, K. Kim, Q.-H.Park, "Performance analysis and optimization of three-dimensional FDTD on GPU using roofline model," J. Comput.Phys. Commun., 182, 2011, pp.1201-1207.

11. D. De Donno, A. Esposito, L. Tarricone, L. Catarinucci, "Introduction to GPU Computing and CUDA Programming: A Case Study on FDTD," IEEE Antennas and Propagation Magazine, 52, 3, 2010, pp. 116-122.

12. M. Livesey, J. F. Stack, F. Costen, T. Nanri, N. Nakashima, S. Fujino, "Development of a CUDA Implementation of the 3D FDTD Method," IEEE Antennas and Propagation Magazine, 54, 5, 2012, pp. 186-195.

13. M. Unno, S. Aono, and H. Asai, "GPU-Based Massively Parallel 3-D HIE-FDTD Method for High-Speed Electromagnetic Field Simulation," IEEE Transactions on Electromagnetic Compatibility, 54, 4, August 2012, pp. 912-921.

14. G. Çakır, M. Çakır, and L. Sevgi, "A Multipurpose FDTD based Two-dimensional Electromagnetic virtual Tool," IEEE Antennas and Propagation Magazine, 48, 4, August 2006, pp. 142-151.

15. G. Çakır, M. Çakır, and L. Sevgi, "A Novel Virtual FDTDBased Microstrip Circuit Design and Analysis Tool," IEEE Antennas and Propagation Magazine, 48, 6, December 2006, pp. 161-173.

16. M. Çakır, G. Çakır, and L. Sevgi, "A Two-dimensional FDTD-Based Virtual Metamaterial – ave Interaction Visualization Tool," IEEE Antennas and Propagation Magazine, 50, 3, June 2008, pp. 166-175.

17. Ç. Uluışık, G. Çakır, M. Çakır, and L. Sevgi, "Radar Cross Section (RCS) Modeling and Simulation: Part I – A Tutorial
Review of Definitions, Strategies, and Canonical Examples,"IEEE Antennas and Propagation Magazine, 50, 1, February 2008, pp. 115-126.

18. G. Çakır, M. Çakır, and L. Sevgi, "Radar Cross Section (RCS) Modeling and Simulation: Part II – A Novel FDTDBasedRCS Prediction Virtual Tool," IEEE Antennas and Propagation Magazine, 50, 2, April 2008, pp. 81-94.

19. G. Çakır, M. Çakır, and L. Sevgi, "FDTD-Based EMC Virtual Tool for Microstrip Circuits," ELEKTRIK, Turkish Journal of Electrical Engineering and Computer Sciences, 17, 3, December 2009, pp. 315-323.

20. U. F. Knott, Radar Cross Section Measurements, New York, Van Nostrand Reinhold, 1993.

21. D. K. Barton and S. A. Leonov, Radar Technology Encyclopedia,Norwood, MA, Artech House, 1998.

22. L. Sevgi, Complex Electromagnetic Problems andNumerical Simulation Approaches, Piscataway, NJ, IEEEPress/John Wiley & Sons, 2003.

23. L. Sevgi and S. Paker, "FDTD Based RCS Calculations andAntenna Simulations," AEU, International J. of Electron icsand Commun., 52, 2, March 1998, pp. 65-75.

24. L. Sevgi, "Target Reflectivity and RCS Interaction in Integrated Maritime Surveillance Systems Based on Surface WaveHF Radar Radars," IEEE Antennas and Propagation Maga zine,43, 1, February 2001, pp. 36-51.

25. L. Sevgi, "Numerical Simulation Approaches for PhasedArray Design," ACES Journal of Applied ComputationalElectromagnetics Society, 21, 3, November 2006, pp. 206-217.

26. R. J. Luebberset. al. "A Finite-Difference Time-DomainNear Zone to Far Zone Transformation," IEEE Transactions onAntennas and Propagation, AP-39, 4, April 1991, pp. 429-433.

27. R. F. Harrington, Field Computation by Moment Methods,New York, The Macmillan Co., 1968.

28. G. J. Burke and A. J. Poggio, "Numerical ElectromagneticCode-Method of Moments, Part I: Program Description, Theory,Technical Document, 116, Naval Electronics SystemCommand (ELEX 3041), 1977.

29. Visit http://www.nittany-scientifi c.com for NEC-WIN Pro.

30. K. S. Kunz and R. J. Luebbers, The Finite-Difference Time-Domain Method for Electromagnetics, Boca Raton, FL, CRC Press, 1993.

